

RESEARCH PAPER

Synthesis Nanocrystalline Cadmium Sulphide Film and the Influence of Cu Doping on the Physical Characterization

Thoalfiqar Ali Zaker¹, Noora Aziz Alweiy², Ali Mohammed Jabbar³, Khalid Haneen Abass⁴, Nadir Fadhil Habubi⁵, Sami Salman Chiad^{5*}

¹ Department of Physics, Collge of Education, University of Al-Hamdaniya, Al-Hamdaniya, Nineveh, Iraq.

² Department of Medical Physics, Al-Mustaqbal University College, Babylon, Iraq.

³ Department of Physics, College of Science, Mustansiriyah University, Baghdad, Iraq.

⁴ Department of Physics, College of Education for Pure Sciences, University of Babylon, Iraq.

⁵ Department of Physics, Collge of Education, Mustansiriyah University, Baghdad, Iraq.

ARTICLE INFO

Article History:

Received 15 January 2021

Accepted 15 March 2021

Published 01 April 2021

Keywords:

AFM

Band gab

CdS Thin Films

Spray pyrolysis

UV

XRD

ABSTRACT

A thin film is a layer of material ranging from fractions of a nanometer to several micrometers in thickness. The controlled production of materials as thin films is a crucial step in many applications. In this work, CdS thin films were prepared by spray pyrolysis procedure at temperature 450 oC. The XRD, AFM and UV-Visible analysis were utilized to investigate the CdS films. The XRD investigation showed that prepared thin films have hexagonal structure with a particular direction along (101) plane. The crystallite size was measured from X-ray diffraction utilizing Scherrer's equation. Atomic force microscopy (AFM) confirmed that the grain was consistently disseminated over the outside of the substrate for the CdS films. The grain size of the nanoparticles were calculated 66.26, 57.11 and 56.52 nm for the CdS, CdS :2% Cu, CdS :4% Cu respectively. The optical properties were done utilizing the UV-Visible analysis. It is found that Cu content affect the optical properties and via increasing the Cu amount, the band gap was decreased.

How to cite this article

Zaker T.A., Alweiy N.A., Jabbar A.M., Abass K.H., Habubi N.F., Chiad S.S. Synthesis Nanocrystalline Cadmium Sulphide Film and the Influence of Cu Doping on the Physical Characterization . J Nanostruct, 2021; 11(2): 269-275. DOI: 10.22052/JNS.2021.02.007

INTRODUCTION

Several technologies are currently used to reduce materials into nano-sizes and nano-thickness, resulting in the emergence of new and unique behaviors [1-5]. There are several ways that thin films differ from bulk materials with the same chemical composition due to their high surface-to-volume ratios [6-8]. It should be noted that all materials, such as thin films, are either amorphous or polycrystalline depending on the preparation conditions and material characteristics [9, 10]. Thin films consist of two parts: the layer under the film

and the substrate [11]. Many electronic devices rely on semiconductor materials, which include silicon, gallium arsenide, and cadmium sulfide [12-15]. A strong absorption in Cadmium Sulphide has attracted researchers because it is used in the fabrication of optoelectronic and photoconductive devices. The band gap of CdS is about 2.42 eV to 2.5 eV at room temperature [16, 17]. It is possible to grow CdS films in both hexagonal (wurtzite) and cubic (zinc blende) phases [18, 19]. Cadmium sulfide thin films are suitable for the window layer of CdTe/CdS heterojunction solar cells. Highly efficient solar cells require uniform and transparent

* Corresponding Author Email: dr.sami@uomustansiriyah.edu.iq

CdS thin films [20-22]. Among the properties that depend on size are: melting point at 400 °C at 2.5 nm, phase transformation at a high pressure from wurtzite to rock salt cubic phase. CdS thin films have been prepared through a variety of methods, including chemical bath deposition, vacuum evaporation, thermal evaporation, RF sputtering, electron beam evaporation, and pulsed laser deposition. Scientists conduct research on doped CdS thin films because of their significant merits with regard to self-quenching, sufficient thermal and photochemical features, and larger Stokes shift [16, 23].

F.T. Munna et al. prepared zinc-doped cadmium sulfide thin films via chemical bath deposition-grown. Thiourea (NH_2SCNH_2) and N-methylthiourea ($\text{NH}_2\text{CSNHCH}_3$) were applied as a sulfur source. The impact of Zn^{2+} doping on as-grown CdS films was investigated. The optical transmittance increases as the zinc content rises, according to the findings. As a sulphur source, thiourea has an optical bandgap of 2.35 eV to 2.45 eV, and N-methylthiourea has a bandgap of 2.2 eV to 2.4 eV [24].

In another work, the CdS thin films were prepared by close spaced sublimation at a temperature of 550°C under vacuum for varying periods of time. For Cu doping of as-deposited thin films, copper nitrate solution was immersed in an 80 ± 5 °C solution for various durations. It is found with increasing copper immersion time, copper transmittance falls from 80% to 30% [25].

In this study, copper doped CdS thin films was synthesized via pyrolysis procedure strategy. The morphological, optical and electrical properties of the as-prepared thin films were characterized comprehensively. The effect of copper on the physical properties of cadmium sulfide thin film was investigated.

MATERIALS AND METHODS

Cu-doped CdS was grown using the simple and fast chemical procedure. Cadmium chloride (CdCl_2) (Supplied from BDH Chemicals, UK) and thiourea [$(\text{NH}_2)_2\text{CdS}$] (provided from Merck Chemicals, India) were dissolved in distilled water to prepare CdS thin films grown on glass substrate and then heated at 450 °C. The copper chloride (provided from TCI Chemicals, India) was added to this system with 2% and 4% as a dopant for providing CdS:Cu thin film. The optimum conditions were applied as following; spraying rate was 5 ml/min, distance

between spout and substrate was around 29 cm, showering rate was adjusted 9 s followed by 2 min hold back to maintain a strategic distance from over the top substrate cooling and transporter gas was Nitrogen. The got films were adherent, free from pinholes and with sensible film homogeneity. Films thicknesses were measured by gravimetric strategy and was in the scope of 325 ± 30 nm. The basic properties of CdS:Cu thin films were done utilizing X-ray diffractometer. Surface geography of the as kept films was acquired by AFM (AA 3000 Scanning Probe Microscope). The UV-Vis spectrophotometer (SHIMADZU UV-2450) was utilized to investigation the optical properties at the range of 200–800 nm.

RESULT AND DISCUSSION

Fig. 1, displays the XRD of the prepared films. A peak situated at 36.79° attributed to the (101) plane of the hexagonal structure. With additional expanding in the statement at doping in 2% and 4% CdS: Cu, the peak identified with the plane (101) became better and extreme. These outcomes in concurrence with the standard CdS X-ray diffraction information document [No. 43-089 JCPDS prevalent]. The hexagonal particular direction (101), as for our situation, has been accounted for CdS thin films grown by pyrolysis.

The crystallite size (D) was determined utilizing Debye-Scherrer formula:

$$D = \frac{0.9\lambda}{\beta \cos\theta} \quad (1)$$

$$\delta = \frac{1}{D^2} \quad (2)$$

$$\varepsilon = \frac{\beta \cos\theta}{4} \quad (3)$$

while, the separation thickness boundary diminished from 2.69 to 2.32, the strain (%) boundary diminished from 6.02 to 4.49 with Cu fixation as recorded in Table. 1

Fig. 2 shows the FWHM, Grain size, Dislocation thickness and Strain of the prepared films. The crystallite sizes were increased via increasing Cu content in prepared thin films.

Fig. 3 shows three dimensional AFM micrograph of the CdS thin films. The images show all around characterized molecule like highlights with granular morphology and demonstrate the presence of little translucent grains. The AFM

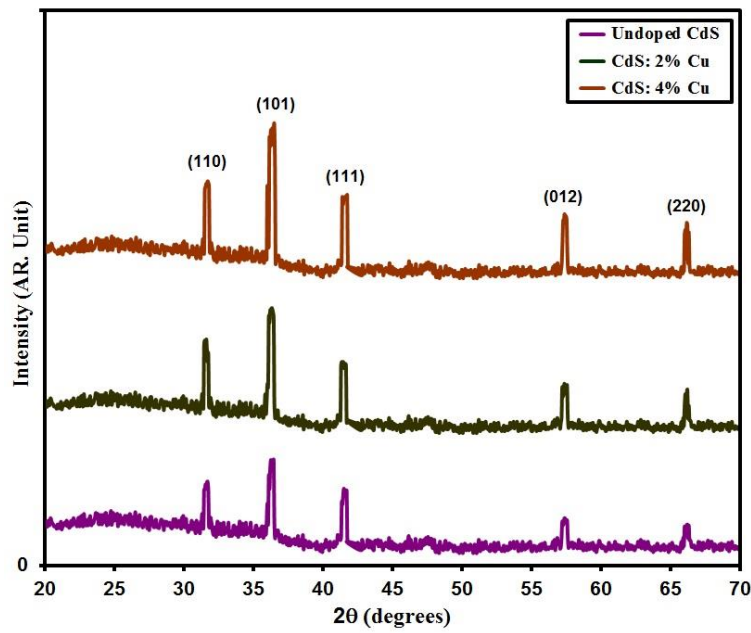


Fig. 1. XRD-patterns of the grown films.

Table 1. Grain size, optical band gap and structural parameters of the prepared films.

Samples	(hkl) Plane	2θ (°)	FWHM (°)	Grain size (nm)	Optical bandgap (eV)	Dislocations density ($\times 10^{15}$)(lines/m ²)	Strain $\times 10^{-3}$
CdS pure	101	36.79	0.65	12.88	2.42	6.02	2.69
CdS: 2% Cu	101	36.45	0.60	13.94	2.36	5.14	2.48
CdS: 4% Cu	101	36.02	0.56	14.92	2.31	4.49	2.32

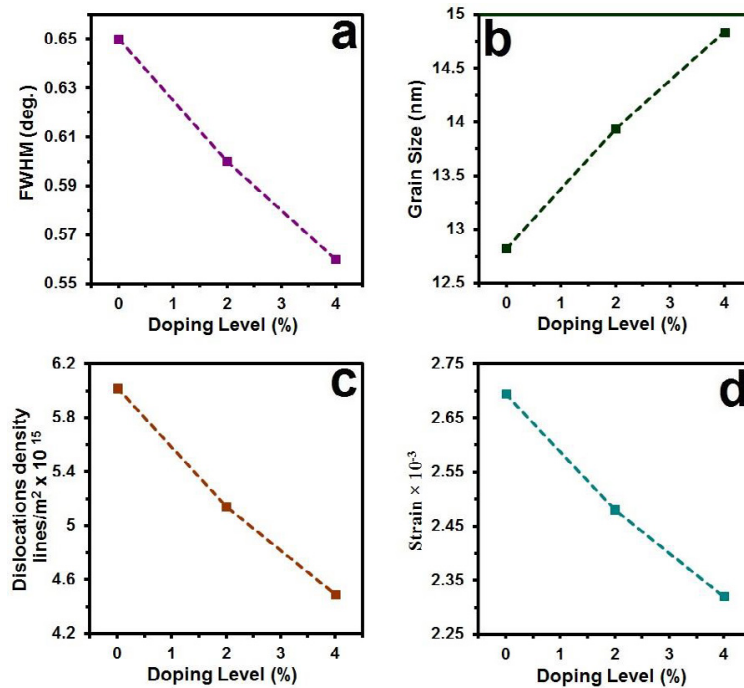


Fig. 2. FWHM (a) Grain size (b) Dislocation (c) Strain (d) of the prepared films.

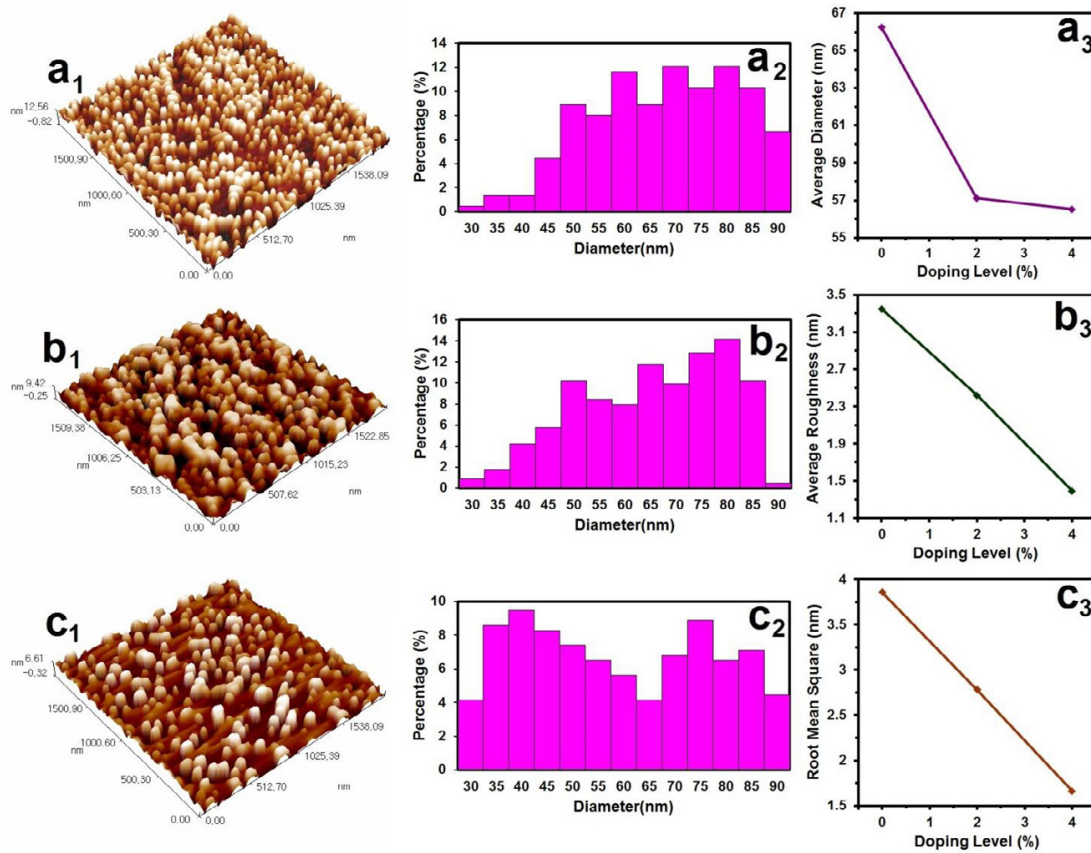


Fig. 3. AFM images of the prepared films (a1, b1 and c1), granularly distributed (a2, b2 and c2) and variation of AFM parameters via doping (a3, b3 and c3).

Table 2. AFM parameters of the deposited films.

Samples	Average Particle size nm	Roughness Average (nm)	R. M. S. (nm)
CdS pure	66.26	3.35	3.86
CdS: 2% Cu	57.11	2.42	2.78
CdS: 4% Cu	56.52	1.39	1.66

analysis additionally revealed a homogeneous structure of films with no breaks and is constant with all around associated grains. Table 2 shows the estimations of normal harshness and root mean square surface roughness (RMS) of as kept and strengthened films. The results were in good agreement with Hasoon et. al. [48]. As can be seen the Cu doping can be have a significant effects on the roughness average and RMS. The surface morphology of the samples has been studied by utilizing nuclear power magnifying lens (AFM). The grain size of the nanoparticles was showed in the scope of 66.26, 57.11 and 56.52 nm for the (CdS, CdS :2% Cu, CdS :4% Cu) respectively.

The Rrms estimation of 3.86 nm for as kept CdS thin films diminished to 1.66 nm by diminished of doping, Ra roughness boundaries as a component of dopant fixation were given in Fig. 3 (a₃, b₃, and c₃) separately. Table 2 represents the estimations of AFM parameters.

The transmission spectra of as-obtained products have appeared in Fig. 4. It was revealed that the transmission shifted from 80 to 95% in visible region. Accordingly, CdS is considered as a glass material for the obvious just as the infrared region.

The absorption coefficient (α) was determined from equation :

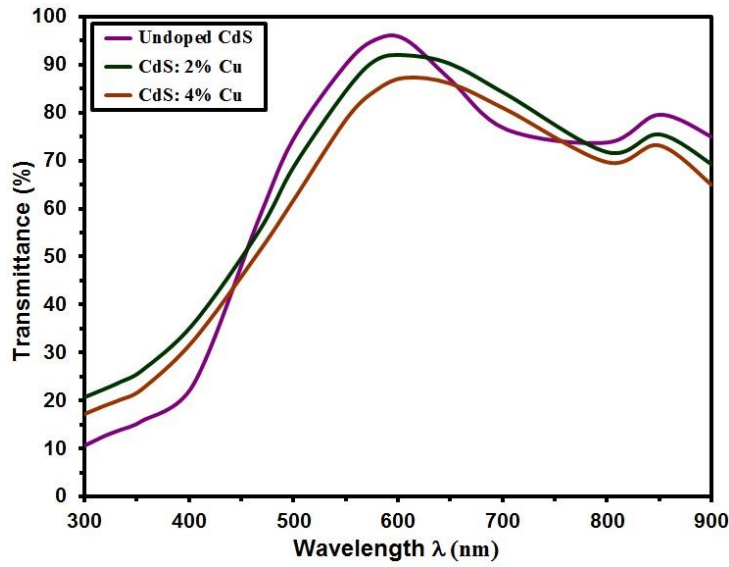


Fig. 4. Transmittance for the prepared films.

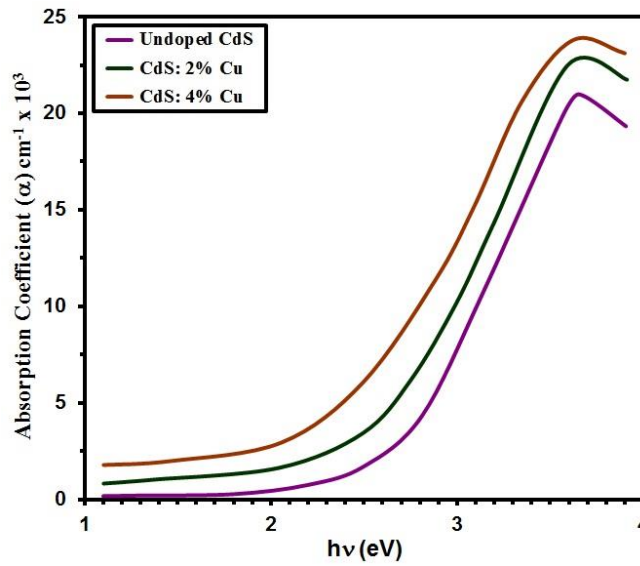


Fig. 5. α Vs $h\nu$ of the prepared thin films

$$\alpha = (2.303 \times A) / t \quad (4)$$

Where (t) is film thickness, A is absorbance. Fig. 5 confirmed that α diminished with an increasing at 2% or 4% doping.

The optical band gap was calculated for pure CdS and doped thin films by:

$$(\alpha h\nu) = A(h\nu - E_g)^{(1/2)} \quad (5)$$

Where A is constant, E_g is the energy gap, $h\nu$ is photon energy. The optical band gap can be acquired by extra plotting the direct bit of the plot $(\alpha h\nu)^2$ versus $h\nu$. The bandgap estimation was estimated from the plot $(\alpha h\nu)^2$ against $h\nu$ as appeared in Fig. 6. As well as shown, the optical band gap were determined as 2.42, 2.36, and 2.31 eV for pure CdS, 2%Cu-doped CdS, and 4%Cu-doped CdS respectively.

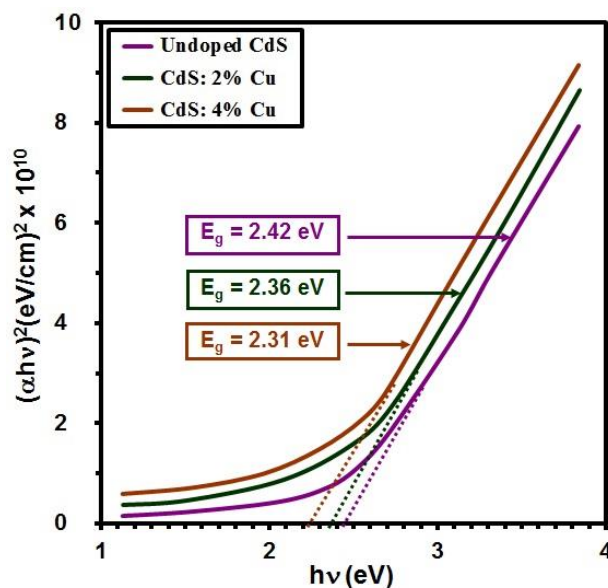


Fig. 6. $(\alpha hv)^2$ Vs $h\nu$ of the prepared thin films.

CONCLUSION

In this work, the CdS films were prepared via various Cu dopants via simple and fast chemical route. XRD analysis confirmed that obtained thin films have hexagonal structure with the particular direction along the plane (101). structural examinations demonstrated that normal grain size increased from 12.88 nm to 14.92 nm with increment in Cu content in thin films (CdS, CdS :2% Cu, CdS :4% Cu). The surface morphology has been studied by utilizing nuclear power magnifying lens (AFM). The grain size of the nanoparticles were calculated 66.26, 57.11, and 56.52 nm for the CdS, CdS :2% Cu, CdS :4% Cu respectively. The transmittance spectra have been recorded, which indicated that the absorption edges of CdS thin film varied at various Cu doping. The calculated optical band gap has been decreased from 2.42 to 2.31 eV via Cu doping.

ACKNOWLEDGMENTS

This work was supported by Mustansiriyah University (www.uomustansiriyah.edu.iq), College of Education, Baghdad, Iraq.

CONFLICT OF INTEREST

The authors declare that there is no conflict of interests regarding the publication of this manuscript.

REFERENCES

1. Asha AB, Narain R. Chapter 15 - Nanomaterials properties. In: Narain R, editor. *Polymer Science and Nanotechnology*; Elsevier; 2020. p. 343-359.
2. Mishra PK. Aggregation of a macromolecule in a nano cube. *Materials Today: Proceedings*. 2020.
3. Shalaby MS, Abdallah H, Chetty R, Kumar M, Shaban AM. Silver nano-rods: Simple synthesis and optimization by experimental design methodology. *Nano-Structures & Nano-Objects*. 2019;19:100342.
4. Shehabeldine A, Hasanin M. Green synthesis of hydrolyzed starch-chitosan nano-composite as drug delivery system to gram negative bacteria. *Environmental Nanotechnology, Monitoring & Management*. 2019;12:100252.
5. Yu K, Liang Y, Ma G, Yang L, Wang T-J. Coupling of synthesis and modification to produce hydrophobic or functionalized nano-silica particles. *Colloids and Surfaces A: Physicochemical and Engineering Aspects*. 2019;574:122-30.
6. Pukenas A, Chekhonin P, Meißner M, Hieckmann E, Aswartham S, Freudenberger J, et al. Direct study of structural phase transformation in single crystalline bulk and thin film BaFe2As2. *Micron*. 2019;119:1-7.
7. Arumugam K, Chen H-M, Dai J-H, Gao M-F, Goyal A, Lin M-K, et al. Using irradiation effect to study the disparate anchoring stabilities of polar-organic molecules adsorbed on bulk and thin-film metal surfaces. *Applied Surface Science*. 2019;493:1090-7.
8. Yu S, Zhao L, Liu R, Wu M, Sun Y, Li L. Electrical properties of bulk and interface layers in Sb doped SnO2 thin films. *Ceramics International*. 2019;45(2):2201-6.
9. Sepulveda J, Villegas C, Torres A, Vargas E, Rodriguez F, Baltazar S, et al. Effect of functionalized silica nanoparticles on the mass transfer process in active PLA nanocomposite films obtained by supercritical impregnation for sustain-

- able food packaging. *The Journal of Supercritical Fluids*. 2020;161:104844.
10. Meisner LL, Rotshtein VP, Semin VO, Meisner SN, Markov AB, Yakovlev EV, et al. Microstructural characterization and properties of a Ti-Ta-Si-Ni metallic glass surface alloy fabricated on a TiNi SMA substrate by additive thin-film electron-beam method. *Surface and Coatings Technology*. 2020;404:126455.
 11. Westmacott K, Weng B, Wallace GG, Killard AJ. Nanostructured conducting polymers for electrochemical sensing and biosensing. *Nanosensors for Chemical and Biological Applications*: Elsevier; 2014. p. 150-94.
 12. Mokkalapati S, Saxena D, Tan HH, Jagadish C. Semiconductor Nanowire Optoelectronic Devices. *Semiconductors and Semimetals*: Elsevier; 2016. p. 1-15.
 13. Wang S, Wang Q, Liu Y, Jia L, Yu M, Sun P, et al. Low-loss through silicon Vias (TSVs) and transmission lines for 3D optoelectronic integration. *Microelectronic Engineering*. 2021;238:111509.
 14. Gallium arsenide for micro and optoelectronic. *III-Vs Review*. 1993;6(4):59.
 15. Ozga K, Yanchuk OM, Tsurkova LV, Marchuk OV, Urubkov IV, Romanyuk YE, et al. Operation by optoelectronic features of cadmium sulphide nanocrystallites embedded into the photopolymer polyvinyl alcohol matrices. *Applied Surface Science*. 2018;446:209-14.
 16. El Kissani A, Ait Dads H, Oucharrou S, Welatta F, Elaakib H, Nkhaili L, et al. A facile route for synthesis of cadmium sulfide thin films. *Thin Solid Films*. 2018;664:66-9.
 17. Mendivil Palma MI, Krishnan B, Avellaneda DA, Martínez Guerra E, Shaji S. Effect of wavelengths on the structure, morphology and optoelectronic properties of cadmium sulfide thin films by laser assisted chemical bath deposition. *Materials Today: Proceedings*. 2020;33:1434-43.
 18. Márquez-Marín J, Torres-Castanedo CG, Torres-Delgado G, Aguilar-Frutos MA, Castanedo-Pérez R, Zelaya-Ángel O. Very sharp zinc blende-wurtzite phase transition of CdS nanoparticles. *Superlattices and Microstructures*. 2017;102:442-50.
 19. Edossa TG, Woldemariam MM. Electronic, Structural, and Optical Properties of Zinc Blende and Wurtzite Cadmium Sulfide (CdS) Using Density Functional Theory. *Advances in Condensed Matter Physics*. 2020;2020:1-8.
 20. Willars-Rodríguez FJ, Chávez-Urbiola IR, Hernández-Landaverde MA, Vorobiev P, Ramírez-Bon R, Vorobiev YV. Effects of tin-doping on cadmium sulfide (CdS:Sn) thin-films grown by light-assisted chemical bath deposition process for solar photovoltaic cell. *Thin Solid Films*. 2018;653:341-9.
 21. Veerathangam K, Pandian MS, Ramasamy P. Size-dependent photovoltaic performance of cadmium sulfide (CdS) quantum dots for solar cell applications. *Journal of Alloys and Compounds*. 2018;735:202-8.
 22. Cao A, Tan T, Zhang H, Du Y, Sun Y, Zha G. Electronic structures and optical properties of the CdTe/CdS heterojunction interface from the first-principles calculations. *Physica B: Condensed Matter*. 2018;545:323-9.
 23. Jayaramaiah JR, Jayanth V, Shamanth R. Structural elucidation and optical analysis on europium doped cadmium sulphide nano thin films. *Optik*. 2020;208:164079.
 24. Munna FT, Chelvanathan P, Sobayel K, Nurhafiza K, Sarkar DK, Nour M, et al. Effect of zinc doping on the optoelectronic properties of cadmium sulphide (CdS) thin films deposited by chemical bath deposition by utilising an alternative sulphur precursor. *Optik*. 2020;218:165197.
 25. Shah NA, Sagar RR, Mahmood W, Syed WAA. Cu-doping effects on the physical properties of cadmium sulfide thin films. *Journal of Alloys and Compounds*. 2012;512(1):185-9.